

1965

Turbulent Mixing and Heat Exchange in a Parallel Stream of Air

Tek Chand Goel

Follow this and additional works at: <https://openprairie.sdstate.edu/etd>

Recommended Citation

Goel, Tek Chand, "Turbulent Mixing and Heat Exchange in a Parallel Stream of Air" (1965). *Electronic Theses and Dissertations*. 3046.
<https://openprairie.sdstate.edu/etd/3046>

This Thesis - Open Access is brought to you for free and open access by Open PRAIRIE: Open Public Research Access Institutional Repository and Information Exchange. It has been accepted for inclusion in Electronic Theses and Dissertations by an authorized administrator of Open PRAIRIE: Open Public Research Access Institutional Repository and Information Exchange. For more information, please contact michael.biondo@sdstate.edu.

TURBULENT MIXING AND HEAT EXCHANGE IN A PARALLEL
STREAM OF AIR

BY

TEK CHAND GOEL

A thesis submitted
in partial fulfillment of the requirements for the
degree Master of Science, Major in
Mechanical Engineering, South
Dakota State University

1965

~~SOUTH~~ DAKOTA STATE UNIVERSITY LIBRARY

TURBULENT MIXING AND HEAT EXCHANGE IN A PARALLEL
STREAM OF AIR

This thesis is approved as a creditable and independent investigation by a candidate for the degree, Master of Science, and is acceptable as meeting the thesis requirements for this degree, but without implying that the conclusions reached by the candidate are necessarily the conclusions of the major department.

Thesis Adviser

Dec. 11, 1964
Date

Head, Mechanical Engineering
Department

Dec. 11, 1964
Date

ACKNOWLEDGMENTS

The author wishes to express his appreciation and gratitude to Professor John F. Sandfort for his guidance and counselling throughout the author's graduate work and in the preparation of this thesis.

The author wishes to thank Dr. William L. Tucker for his assistance in compiling the computer program and for making the computer available for this project.

The author wishes to thank the Engineering Experiment Station of South Dakota State University for financing this project.

TCG

2011

TABLE OF CONTENTS

Chapter	Page
I. INTRODUCTION	1
II. BACKGROUND ON TURBULENCE	3
Definition of Turbulence	3
Development of Reynold's Stresses	3
Correlation of Fluctuating Components	5
III. REVIEW OF THE LITERATURE	7
IV. TEST FACILITIES	13
Description of Wind Tunnel	13
Electronic Equipment	17
Equipment for Temperature Measurement	18
V. TEST PROCEDURE	21
VI. ANALYSIS OF RESULTS	23
Mean Velocity Distribution	23
Temperature Distribution	26
Intensity of Turbulence	35
VII. CONCLUSIONS AND RECOMMENDATIONS	41
Summary of Results	41
Recommendations	42
LITERATURE CITED	44
APPENDIX A	46
APPENDIX B	48
APPENDIX C	50
APPENDIX D	52

LIST OF TABLES

Table		Page
1.	Velocity and Temperature Distribution for Turbulent Streams of Equal Velocities	52
2.	Velocity and Temperature Distribution for Turbulent Streams of Equal Velocities	53
3.	Velocity and Temperature Distribution for Turbulent Streams of Unequal Velocities	54
4.	Intensity of Turbulence for Streams of Equal Velocities	55

LIST OF FIGURES

Figure	Page
I. Wind tunnel schematic diagram	14
II. Velocity profile at $X = 0$	16
III. Temperature probe	19
IV. Velocity distribution for turbulent streams of equal velocities	24
V. Temperature distribution for turbulent streams of equal velocities and different densities	27
VI. Velocity distribution for turbulent streams of equal velocities	28
VII. Temperature distribution for turbulent streams of equal velocities and different densities	29
VIII. Velocity distribution for turbulent streams of unequal velocities	30
IX. Mixing boundaries of heat and momentum	31
X. Recovery of minimum velocity at the center of splitter plate	32
XI. Intensity of turbulence for streams of equal velocities	37
XII. Intensity of turbulence for streams of equal velocities	38
XIII. Dissipation of intensity of turbulence at the center of splitter plate	39
XIV. Hot-wire probe calibration curve	47

NOMENCLATURE

- C_p = specific heat, BTU per lb per degree F
- g = gravitational acceleration, 32.2 ft/sec^2
- I = hot-wire current, milliamperes
- I_0 = hot-wire current at zero velocity, milliamperes
- I_C = square-wave current, milliamperes
- J = mechanical equivalent of heat, ft-lb per BTU
- L = mixing length
- L_w = mixing length
- M_1 = random signal voltmeter reading, hot-wire heated, millivolts
- M_2 = random signal voltmeter reading, hot-wire unheated, millivolts
- M_3 = random signal voltmeter reading, hot-wire heated and square wave superimposed, millivolts
- P = static pressure, psig
- \bar{P} = mean static pressure
- P' = fluctuating static pressure
- P_{abs} = absolute pressure, psia
- ρ = density
- $R_{U'V'}$ = correlation coefficient of longitudinal and transverse components
- $R_{U_1U_2}$ = longitudinal correlation coefficient
- t = time
- T = temperature in the mixing region, degree F
- T_S = stagnation temperature, degree F
- T_{max} = maximum free stream temperature, degree F

U = velocity in the X direction

\bar{U} = mean velocity in the X direction, feet per second

U' = fluctuating velocity in the X direction

U_A = free stream mean velocity in stream "A," feet per second

U_B = free stream mean velocity in stream "B," feet per second

U_{\max} = maximum free stream mean velocity, feet per second

$\frac{\sqrt{U'^2}}{\bar{U}}$ = longitudinal intensity of turbulence

μ = viscosity

V = velocity in the Y direction

\bar{V} = mean velocity in the Y direction

W = velocity in the Z direction

\bar{W} = mean velocity in the Z direction

W' = fluctuating velocity in the Z direction

X = longitudinal coordinate in the direction of flow, $X = 0$ corresponds to the location where streams start to mix

Y = lateral coordinate in the transverse direction of flow, $Y = 0$ corresponds to the center of splitter plate

Z = lateral coordinate perpendicular to XY plane

CHAPTER I

INTRODUCTION

Turbulent mixing of air, gases of different densities, and gases of different kinds are of fundamental importance to scientists and mathematicians, and are of practical importance to engineers. Turbulence as it occurs in nature is of mysterious nature, and there are insurmountable mathematical difficulties in completely analyzing the mechanism by which it is produced. While theoretical researchers are busy finding new ways and means to solve turbulence problems, the practical researchers have been successful in gaining more insight into turbulence phenomena by applying semi-empirical theories. With the invention of the hot-wire anemometer, it has been possible to measure in wind tunnels, the intensity of turbulence, the correlation of longitudinal and transverse fluctuating components, the microscale and macroscale of small and large eddies, and the turbulence spectrum. Recently, with the availability of hot-wire anemometer on a commercial basis, we have been able to investigate turbulence phenomena that previously were confined to more specialized research centers.

When parallel streams of air, divided by a flat plate, are allowed to mix, the mixing boundaries are extensions of the boundary layer initially developed upstream of the mixing zone. As the stream leaves the separating plate, zero velocity at the plate suddenly disappears. Momentum from the potential flow is transferred to the

boundary layer, and the continuous transfer of energy causes a lateral growth of the boundary layer in the mixing zone. This growth of the mixing region boundaries would continue indefinitely except for the eventual containment of the confining walls.

The purpose of this investigation was to study experimentally, the mean velocity distribution, the intensity of turbulence, and the temperature distribution (when one stream is heated) in the mixing zone of two turbulent parallel streams of air.

A hot-wire anemometer and a random signal voltmeter were used to measure the mean velocity and the intensity of turbulence. A copper-constantan thermocouple was used to measure temperature. A special subsonic wind tunnel was already available for this project, and only required a few design modifications to make it suitable for this project.

CHAPTER II

BACKGROUND ON TURBULENCE

Definition of Turbulence

When the fluid particles are traveling in a straight line and orderly manner, it is called laminar flow. When the Reynold's number exceeds 2000, this well ordered and parallel flow ceases. In this case there is superimposed on the main motion in the direction of the axis of the pipe, a subsidiary motion at right angles to it which effects mixing. This irregular motion of the fluid particles is called turbulence. The motion is random in nature. Due to its inherent property of randomness, turbulence as measured is only useful when its average is taken over a finite time.

When a fluid is passing over a surface, the wake behind the body consists of a number of whirling motions which are generally called vortices. Then after the fluid has progressed a certain distance, these vortices decompose into the random motion of turbulence.

Turbulence may be defined as being homogenous when its scale and intensity are independent of the coordinate position. It is further defined as being isotropic when the intensity of turbulent fluctuations are the same in all directions.

Development of Reynold's Stresses

To gain more insight into the phenomena of turbulence, and to make a mathematical representation, it is convenient to separate the

velocity into mean velocity, and the turbulent velocity fluctuating about the mean velocity. The velocity and pressure can be represented in the following form:¹

$$(1) \quad \begin{aligned} U &= \bar{U} + U' \\ V &= \bar{V} + V' \\ W &= \bar{W} + W' \\ P &= \bar{P} + P' \end{aligned}$$

Where \bar{U} denotes temporal average of velocity, and U' denotes fluctuating or turbulent components.

The Navier-Stokes equation can be written in the following form:²

$$(2) \quad \rho \left[\frac{\partial U}{\partial t} + \frac{\partial (U^2)}{\partial x} + \frac{\partial (UV)}{\partial y} + \frac{\partial (UW)}{\partial z} \right] = - \frac{\partial P}{\partial x} + \mu \nabla^2 U$$

$$(3) \quad \rho \left[\frac{\partial V}{\partial t} + \frac{\partial (VU)}{\partial x} + \frac{\partial (V^2)}{\partial y} + \frac{\partial (VW)}{\partial z} \right] = - \frac{\partial P}{\partial y} + \mu \nabla^2 V$$

$$(4) \quad \rho \left[\frac{\partial W}{\partial t} + \frac{\partial (WU)}{\partial x} + \frac{\partial (WV)}{\partial y} + \frac{\partial (W^2)}{\partial z} \right] = - \frac{\partial P}{\partial z} + \mu \nabla^2 W$$

Where ∇^2 denotes Laplace's operator. By replacing the velocity and the pressure terms in the Navier-Stokes equation by their mean and fluctuating components, and by applying averaging process term by term, the following equations are deduced:

¹H. Schlichting, Boundary Layer Theory, McGraw-Hill Book Company, New York, 1955, p. 370.

²Schlichting, op. cit., p. 372.

$$\begin{aligned}
 (5) \quad \rho \left(\frac{\partial \bar{u}}{\partial t} + \bar{u} \frac{\partial \bar{u}}{\partial x} + \bar{v} \frac{\partial \bar{u}}{\partial y} + \bar{w} \frac{\partial \bar{u}}{\partial z} \right) &= - \frac{\partial \bar{P}}{\partial x} + \mu \nabla^2 \bar{u} \\
 &- \rho \left[\frac{\partial \overline{u'^2}}{\partial x} + \frac{\partial \overline{u'v'}}{\partial y} + \frac{\partial \overline{u'w'}}{\partial z} \right] \\
 (6) \quad \rho \left(\frac{\partial \bar{v}}{\partial t} + \bar{u} \frac{\partial \bar{v}}{\partial x} + \bar{v} \frac{\partial \bar{v}}{\partial y} + \bar{w} \frac{\partial \bar{v}}{\partial z} \right) &= - \frac{\partial \bar{P}}{\partial z} + \mu \nabla^2 \bar{v} \\
 &- \rho \left[\frac{\partial \overline{u'v'}}{\partial x} + \frac{\partial \overline{v'^2}}{\partial y} + \frac{\partial \overline{v'w'}}{\partial z} \right] \\
 (7) \quad \rho \left(\frac{\partial \bar{w}}{\partial t} + \bar{u} \frac{\partial \bar{w}}{\partial x} + \bar{v} \frac{\partial \bar{w}}{\partial y} + \bar{w} \frac{\partial \bar{w}}{\partial z} \right) &= - \frac{\partial \bar{P}}{\partial z} + \mu \nabla^2 \bar{w} \\
 &- \rho \left[\frac{\partial \overline{u'w'}}{\partial x} + \frac{\partial \overline{v'w'}}{\partial y} + \frac{\partial \overline{w'^2}}{\partial z} \right]
 \end{aligned}$$

The above averaging process introduces six new additional terms;

$$\overline{u'^2}, \quad \overline{v'^2}, \quad \overline{w'^2}, \quad \overline{u'v'}, \quad \overline{v'w'}, \quad \overline{u'w'},$$

which are called Reynold's or apparent stresses. The terms; $\overline{u'v'}$, $\overline{v'w'}$, and

$\overline{u'w'}$ are turbulent shearing stresses, as the laminar viscous shearing

stress in turbulent flow is negligible. The other three terms (normal

stresses) are associated with the intensity of turbulence. In

isotropic turbulence, intensity of turbulence is defined as $\sqrt{\overline{u'^2}}/\bar{u}$.

Correlation of Fluctuating Components

The correlation of longitudinal and transverse fluctuations can be measured with two hot-wires arranged in a single probe in the form of x-ray. The correlation coefficient is defined as follows:³

³Schlichting, op. cit., p. 377.

$$(8) \quad R_{U'V'} = \frac{\overline{U'V'}}{\sqrt{\overline{U'^2}} \sqrt{\overline{V'^2}}}$$

This is also termed the shear correlation coefficient since $\overline{U'V'}$ is the turbulent shear.

Turbulent flow has in it a mixture of eddies of all sizes. Large size eddies are associated with low frequency and small size eddies are associated with high frequency. It is very important to measure energy distributed between various size eddies. This can be accomplished by studying the spectral distribution of energy over the frequency range with the aid of a wave analyses and frequency is plotted against percentage of total energy. From this plot, energy distributed in various size eddies can be determined.

The next important analysis thereof in turbulent flow is the determination of the size or scale of eddies. There are two scales in turbulent flow; microscale and macroscale. The microscale is the average of smallest size eddies and the macroscale is the average of largest size eddies. The size of eddies can be determined by measuring the longitudinal correlation coefficient between two longitudinal fluctuating components U_1' , and U_2' at points whose transverse distance is Y . The longitudinal correlation coefficient is defined as follows:⁴

$$(9) \quad R_{U_1'U_2'} = \frac{\overline{U_1'U_2'}}{\sqrt{\overline{U_1'^2}} \sqrt{\overline{U_2'^2}}}$$

⁴Schlichting, op. cit., p. 380.

CHAPTER III

REVIEW OF THE LITERATURE

Tollmien,⁵ in 1926, was the first investigator who worked with the general problem of mixing air streams. He specifically solved the case of a single parallel stream of air, air charging into still air and mixing with it. He started with the equation of motion and made the following assumptions to simplify the solution:

1. Pressure gradient in the flow direction was zero.
2. Initial boundary layer thickness was negligible.
3. Friction due to viscosity was neglected.

With the application of Prandtl's momentum theorem, and introducing the stream function to satisfy the equation of continuity, it was possible to reduce the partial differential equation to an ordinary differential equation. Straight line boundaries of the turbulent mixing zone were found to vary linearly with the axis in the direction of flow.

Kuethé,⁶ in 1935, extended Tollmien's method of analysis to a more complicated case of the turbulent mixing of two streams of air at different velocities. Kuethé used the same general approach as that of

⁵W. Tollmien, Calculation of Turbulent Expansion Processes, N.A.C.A., TM No. 1085, 1945.

⁶A. M. Kuethé, Investigations of Turbulent Mixing Regions Formed by Jets, Journal of Applied Mechanics, Vol. 2, pp. A87-A95, 1935.

Tollmien. Experimental results were in close agreement with the theory. When one stream was allowed to mix with the other stream at zero velocity, the mixing boundaries were unsymmetrical. However, as the zero velocity stream approached the velocity of the other stream, mixing boundaries had a tendency to become symmetrical.

Corrsin,⁷ in 1943, did extensive experimental work on a heated jet of air entering a still air reservoir. The experiments were conducted with a three inch nozzle having an outlet velocity of 70 ft/sec, and a temperature difference of 13°F above the surrounding air. A hot-wire anemometer was used to measure mean velocities and turbulent velocities. Temperatures were measured with copper-constantan thermocouples, and were found to diverge more rapidly than velocities. At any cross section in the direction of flow, fully turbulent flow was observed throughout those areas where the velocity was at least one half the maximum velocity. Maximum velocity was at the center. The velocity and turbulent flow profiles remained similar at distances greater than 20 diameters from the outlet of the nozzle. Experimental velocity and temperature profiles were compared with the theoretical curves based on Prandtl's momentum transfer theory and Taylor's vorticity theory. At any cross section, experiments checked fairly well within the distance of one nozzle diameter, but outside of this region, experimental scatter was too great to enable the points

⁷S. Corrsin, Investigation of Flow in an Axially Symmetrical Heated Jet of Air, N.A.C.A., ACR No. 3L23, #94, 1943.

to be fitted into the theoretical curves. This discrepancy could not be explained.

Abramovich,⁸ in 1944, developed a theory for a plane-parallel free stream of a compressible fluid. His theory was applicable to the following two different cases:

1. Where the mixing boundaries were caused by a stream of air entering the medium at rest, the temperature of the stream was different than that of the surroundings and the velocity was less than half velocity of sound.

2. Where the mixing boundaries were caused by a stream of air entering the medium at rest, but with a velocity equal to the velocity of sound.

Abramovich applied the same approach as Tollmien except that he retained the density function in the equation of motion, and in the continuity equation. Also Taylor's vorticity theorem was preferred over the Prandtl's momentum theorem as it gave better correlation between theory and experimental results of heated jets and heated streams. By lowering the temperature of the stream 60°F below that of the surrounding fluid, and at a velocity below one half the velocity of sound, the mixing region boundaries only increased by 0.7 percent. When the velocity of the stream was increased from a very low velocity

⁸G. N. Abramovich, The Theory of a Free Jet of a Compressible Gas, N.A.C.A., TM No. 1058, March, 1944.

to the velocity of sound, the mixing region boundaries decreased by 1.3 percent.

Liepmann and Laufer,⁹ in 1947, studied the so-called half jet phenomena where one side of the free stream is bounded by a solid boundary. Their experiment covered the case of one moving stream mixing with still air. The initial boundary layer that developed upstream of the mixing region was neglected. The divergence of the mixing boundaries under these restrained conditions varied linearly with the axis in the direction of flow. A two dimensional wind tunnel, 60 by 7.5 inches, was specially designed with suitable screens and honey comb paper mailing tubes, to control the intensity of turbulence. Mean and fluctuating velocities were measured with a hot-wire anemometer. Both longitudinal and transverse intensity of turbulence reached its maximum at the outer edge of the mixing boundaries.

Corrsin and Uberio,¹⁰ in 1949, made further studies of a one inch, round, turbulent jet, mixing with still air. Experiments were also conducted with the jet heated to 570°F. The rate of spread of the heated jet was found to be considerably greater than that of the unheated jet.

⁹H. W. Liepmann and J. Laufer, Investigations of Free Turbulent Mixing, N.A.C.A., TN No. 1257, 1947.

¹⁰S. Corrsin and M. S. Uberio, Further Experiments on the Flow and Heat Transfer in a Heated Turbulent Air Jet, N.A.C.A., TN No. 1865, 1949.

Torda and Stillwell,¹¹ in 1956, released a very comprehensive report on mixing of compressible and incompressible turbulent streams, and turbulent jets. This was the first paper where the effect of the initial boundary layer, developed upstream of the mixing region, was taken into account. The mixing boundaries were assumed to be a continuation of the initial boundary layer. The Von Karman integral concept was used by employing the continuity equation, the momentum equation, and the energy equation. Constant exchange coefficient in the form of $E = K b (U_{\max} - \bar{U})$ was used where K is the dimensionless constant to be determined by experiments, and b is the width of the mixing zone. The experiments showed two important deviations from the previous results. First, the boundaries of the mixing zone were found to be curved rather than to vary linearly with downstream distance from the beginning of mixing. Second, they showed that a sudden change of the viscous mechanism at the end of the separating plate caused a contraction of the mixing zone.

Childs and Associates,¹² in 1962, presented a solution for two dimensional turbulent mixing between parallel jets, when the initial boundary layer was taken into consideration. Starting with the

¹¹T. P. Torda and H. S. Stillwell, Analytical and Experimental Investigations of Incompressible and Compressible Mixing of Streams and Jets, WADC Technical Report 55347, 1956.

¹²M. E. Childs and Associates, Two-Dimensional Turbulent Mixing Between Parallel Jets Considering Effects of Initial Boundary Layer. The University of Washington, Department of Mechanical Engineering, October 16, 1962.

equation of motion, Childs used the method of small perturbation as well as constant exchange coefficient to reduce the equation of motion to the form of the non-steady, one dimensional heat conduction equation. The heat conduction equation was solved for the various boundary layer configurations. In the experimental set up, Childs used a 1/2" wide screen placed perpendicular to the direction of flow. This screen was supposed to thicken the initially boundary layer. The experimental results were in close agreement with the theory.

CHAPTER IV

TEST FACILITIES

Description of Wind Tunnel

A schematic diagram of the wind tunnel is shown in Figure I, and a complete description of the facility is given by Iverson.¹³ The wind tunnel was specially designed to conduct studies on the mixing of turbulent streams of air. A high static pressure fan, manufactured by the New York Blower Company, was powered by a 15 H.P., 3600 RPM 3 phase induction motor. Downstream of the fan outlet, the duct was divided into two streams. There were provisions to regulate the mass rate of flow individually in each stream. U_A/U_B (where U_A is the free stream velocity in stream "A," and U_B is the free stream velocity in stream "B") could be varied from 0.25 to 1.0. Stream "B" was allowed to pass over a steam heating coil as shown in the Figure. The coil was supplied with 15 psig steam which enabled stream "B" to be raised 32°F above the temperature of stream "A." There was a damper at the system outlet, where shown in the Figure I, by which the velocity in the system could be varied from a minimum of 28 feet per second to a maximum of 130 feet per second.

Mean velocities were measured in the wind tunnel during preliminary tests, and it was discovered that the velocity profiles were

¹³R. A. Iverson, The Design of an Apparatus for Investigating Turbulent Mixing of Two Parallel Air Streams and Analysis of Half-Jet Phenomena, M.S. Thesis, South Dakota State University, 1964.

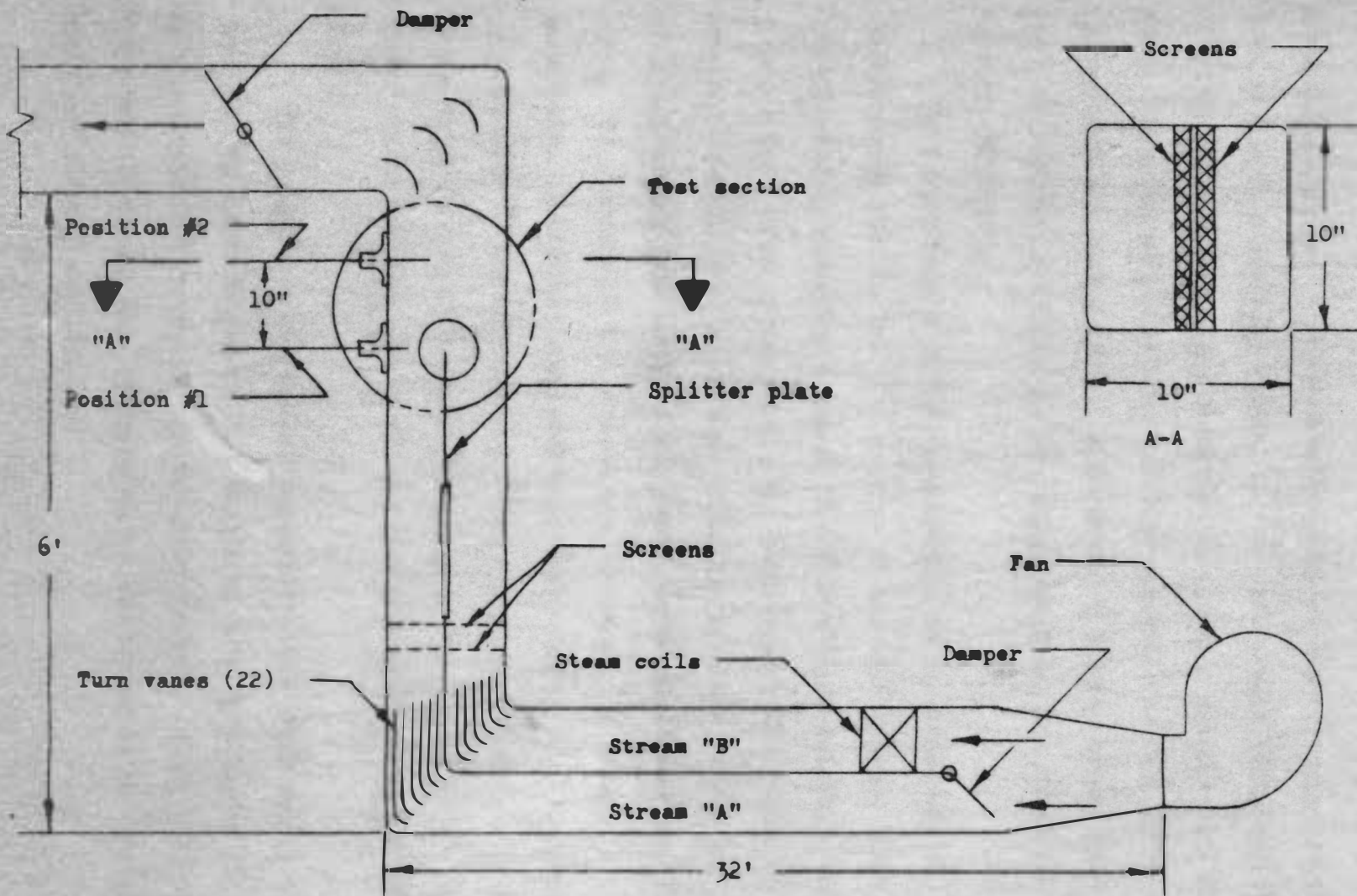


Figure I. Wind tunnel schematic diagram

irregular in shape. A representative plot of the velocity distribution at $X = 0$ is shown in Figure II. As can be seen from Figure II, there is a 20% increase in velocities along the outside radius of the flow. These irregularities in the flow occurred due to a 90° bend upstream of the test section. A distance of 3 feet, between the 90° bend and the test section, was not long enough for the fluid to recover completely.

To further carry on the experiments, it was necessary to stabilize the flow in the test section of the wind tunnel. This was accomplished by designing a new miter elbow with 22 carefully constructed turn vanes at the bend. The turn vanes had 4 inches of straight length in the downstream direction of flow. Also, two screens of 18 meshes per inch, .011" O.D., were placed downstream from turn vanes. The purpose of the screens was to reduce the intensity of turbulence. A 1/2 inch wide ordinary window screen was also installed perpendicular to the direction of flow, and at a distance of 1 1/2 inches from the top of the splitter plate. The purpose of the window screen was to increase the boundary layer thickness along the splitter plate.

The velocity measurements, taken after the above modifications, were plotted again in Figure II. As can be seen from Figure II, there is a definite improvement in the velocity profile. Also, the boundary layer has thickened, and the velocity at the center of the splitter plate has reduced considerably.

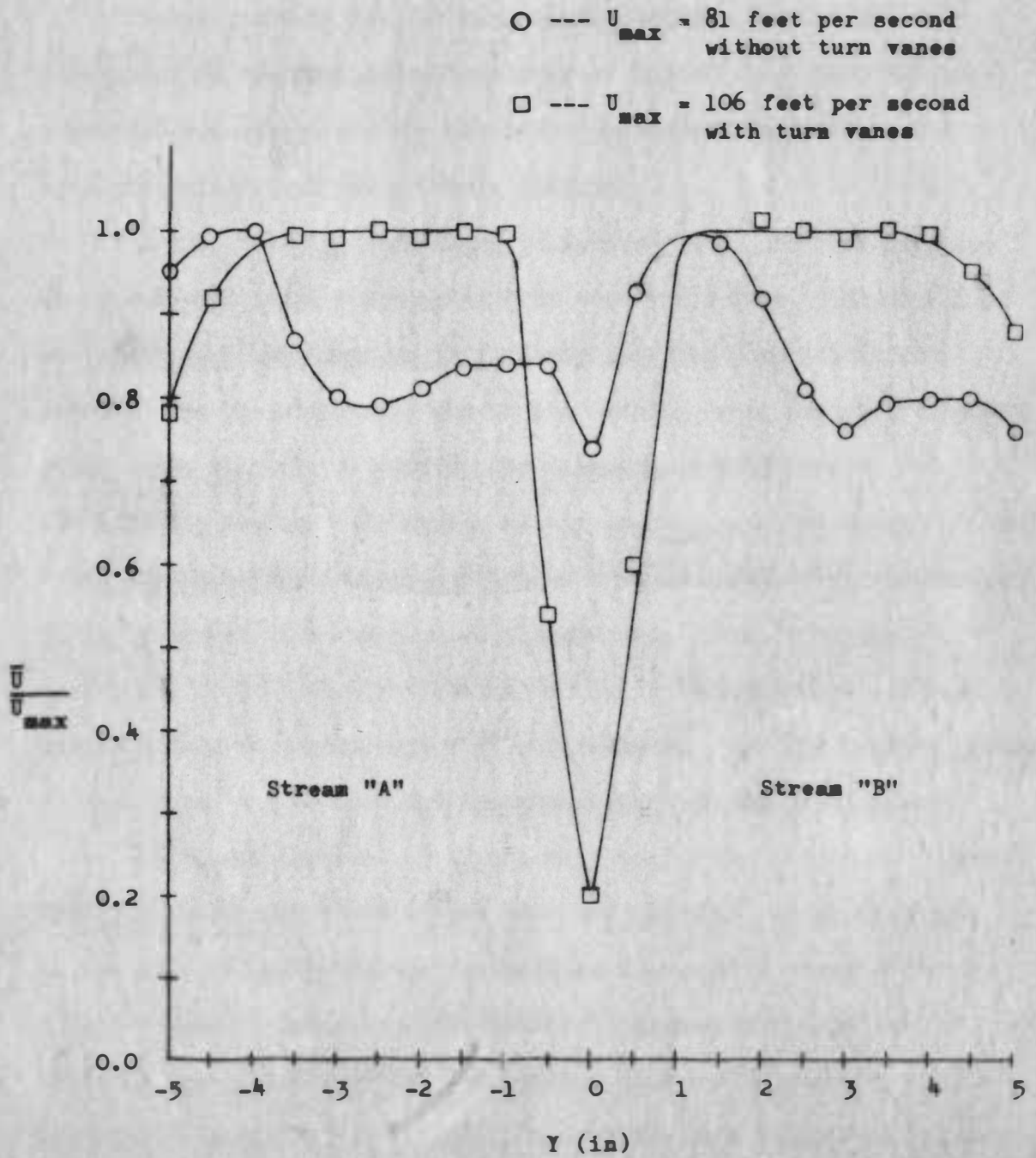


Figure II. Velocity profile at X = 0

Electronic Equipment

Development of the hot-wire anemometer has been of great importance in the fundamental research of turbulence. Both the constant current method and the constant temperature method have been used extensively for the hot-wire circuitry.

A HWB3 hot-wire anemometer, manufactured by the Flow Corporation, was used for the measurement of mean velocities. The design of the instrument was based on the principle of the constant current method. The hot-wire probe had on its working end a tungsten filament which had a diameter of .00035" and a length of .044" and it was electrically heated. The stream of air passing over the heated filament has a cooling effect due to convective heat transfer. The resistance of the filament is a function of temperature. Thus, a change of resistance of the hot-wire filament is due to change in temperature, which in turn is due to change of air velocity. In this manner, change of resistance can be used for the measurement of air velocities.

In the measurement of fluctuating components, it is very important that the temperature of the hot-wire filament should fluctuate at the same frequency as the fluctuating components. However due to a finite thermal inertia of the filament, temperature fluctuations actually lag behind velocity fluctuations and the sensitivity of the instrument is greatly decreased. To increase this sensitivity a compensating circuit is built into the instrument, which automatically corrects for any thermal inertia lag.

A random signal voltmeter, manufactured by the Flow Corporation, was used to measure the turbulent velocities. The voltmeter had an averaging time of 16 seconds which makes it an ideal instrument for the true root-mean-square measurements of random signals.

A DuMont oscilloscope, type 401A, was used for adjusting the compensating frequency for the hot-wire anemometer output signals by the method of square wave calibration. Visual observations of the fluctuating components were made occasionally on the oscilloscope screen.

Equipment for Temperature Measurement

Thermocouple voltage was measured with a Leeds and Northrup, model 8686 potentiometer. The instrument was calibrated against known temperatures. No. 40 copper-constantan wires were used as thermocouple leads, and the thermocouple junction was a ball type welded joint.

The construction of temperature probe is shown in Figure III. Thermocouple wires were wrapped with electrician's tape and threaded into a .04" thick, 1/4" O.D., and 15" long plastic tubing. Plastic material was chosen for its low thermal conductivity, and in this way the heat conducted along the length of the tubing was minimized. The working end of the probe was plugged with a wooden plug. One-fourth inch from the working end; two holes of .045" diameter were drilled 90° apart. The thermocouple junction was aligned with the .045" diameter holes.

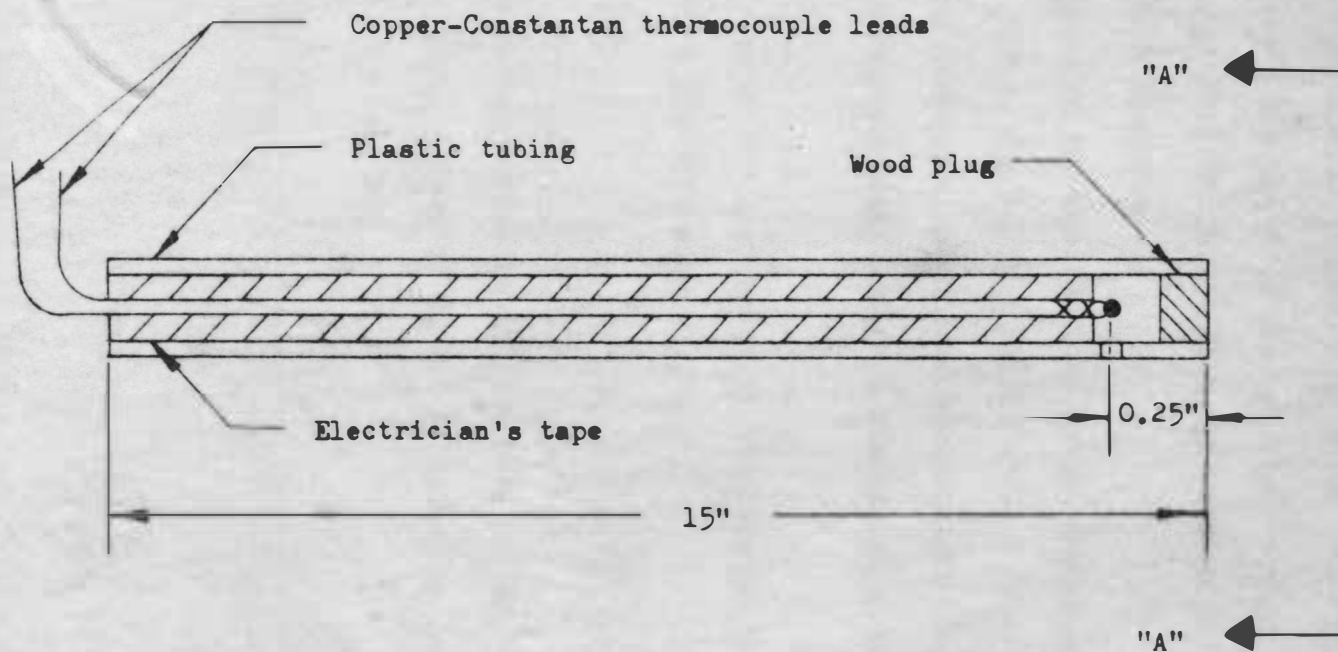
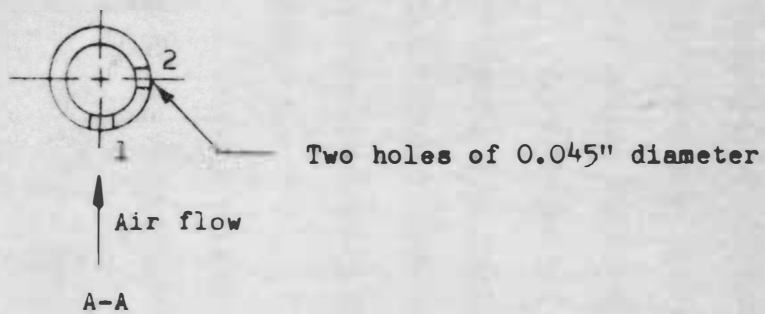


Figure III. Temperature probe

The temperature probe was adjusted in the stream of air in such a way that hole #1 was parallel to the direction of flow. Thus a small sample of air would enter through hole #1, and would escape through hole #2. In this way there would be a constant circulation of air around the thermocouple junction.

A small jet of air passing through the hole would impinge on the thermocouple junction. Thus, due to this impact of air, the kinetic energy which the air possessed would be converted into heat. As a result of this, the instrument would indicate stagnation or total temperature.

The error involved, due to the conversion of the kinetic energy into heat, was calculated from the following equation:¹⁴

$$(10) \quad T = T_S - \frac{\bar{U}^2}{2g J C_p}$$

In this equation, T , T_S , and \bar{U} are variables and the rest of the terms are constants. From the measured values of T_S and \bar{U} , and using the appropriate constants, T was calculated.

¹⁴H. C. Hottel and A. Kalitinsky, Temperature Measurements in High Velocity Air Streams, Journal of Applied Mechanics, Vol. 67, pp. A25-A32, 1949.

CHAPTER V

TEST PROCEDURE

The test probe was threaded into the fitting at position #1 as shown in Figure I. The splitter plate was raised to its maximum position, and was just clearing the probe in the vertical direction. The outlet damper was adjusted at the desired position (full closed to full open). At the full closed position, 20 percent of the mass was still flowing through the system. The splitter damper was adjusted to change the ratio of velocities in the streams. When it was necessary to heat stream "B," gate valve was opened to allow 15 psig steam into the heating coils.

Measurements were made across the width of the duct every 1/2" and close to the splitter plate every 1/4". The splitter plate was lowered to the desired distance and the measurements were again made across the duct width. The procedure was repeated till the splitter plate was at its lowest position. Test probe was then threaded into the fitting at position #2 as shown in Figure I and the procedure was repeated.

For accurate measurements of velocities, I^2 versus $(P_{abs} \bar{U})^{1/2}$ calibration curve was drawn. From the calibration curve, the following equation was derived:¹⁵

¹⁵See Appendix A.

$$(11) \quad \bar{U} = \frac{(I^2 - 3750)^2}{34276.87 P_{abs}}$$

This equation was very convenient for calculating the mean velocities from the measured values of current and pressure. An IBM 1620 digital computer was used for the calculations of velocities. The Fortran program is given in Appendix B.

The intensity of turbulence was computed from the following equation.¹⁶

$$(12) \quad \frac{\sqrt{U'^2}}{\bar{U}} = \frac{4 I_c}{I \left[1 - \left(\frac{I_o}{I} \right)^2 \right]} \sqrt{\frac{M_1^2 - M_2^2}{M_3^2 - M_1^2}}$$

I_c , I_o , I , M_1 , M_2 , and M_3 are measured quantities. These variables are measured with the aid of a random signal voltmeter and a hot-wire anemometer. By using these quantities in the above semi-empirical equation, the intensity of turbulence is calculated.

¹⁶Bulletin No. 37D, Model HWB3 Hot-Wire Anemometer Theory and Instructions, p. 33, Flow Corporation, 205 Sixth Street, Cambridge 42, Massachusetts.

CHAPTER VI

ANALYSIS OF RESULTS

Mean Velocity Distribution

At $X = 0, 6, 11, 16$ and 21 inches, the dimensionless parameter \bar{U}/U_{\max} was plotted against Y in Figure IV, for turbulent streams of equal velocities. X is the coordinate in the direction of flow, Y is the lateral coordinate in the transverse direction, \bar{U} is the mean velocity in the X direction, and U_{\max} is the maximum free stream velocity. Initial readings were taken to equalize the velocities in each stream. The finest adjustment had a maximum free stream velocity of 106 feet per second and 104 feet per second in streams "B" and "A" respectively.

A $1/2$ inch wide ordinary window screen was installed perpendicular to the direction of flow, and at a distance of $1\ 1/2$ inches from the top of the splitter. This was done to widen out the boundary layer at the start of the mixing zone. Further downstream, there was a lateral spread of the boundary layer which can be explained as follows: When the fluid travels along the splitter length, as well as when the fluid leaves the splitter plate, momentum is entrained continuously from the potential flow. This continuous entrainment of momentum, from the potential flow to the boundary layer flow, causes a lateral growth of the boundary layer thickness downstream of the flow. The so called

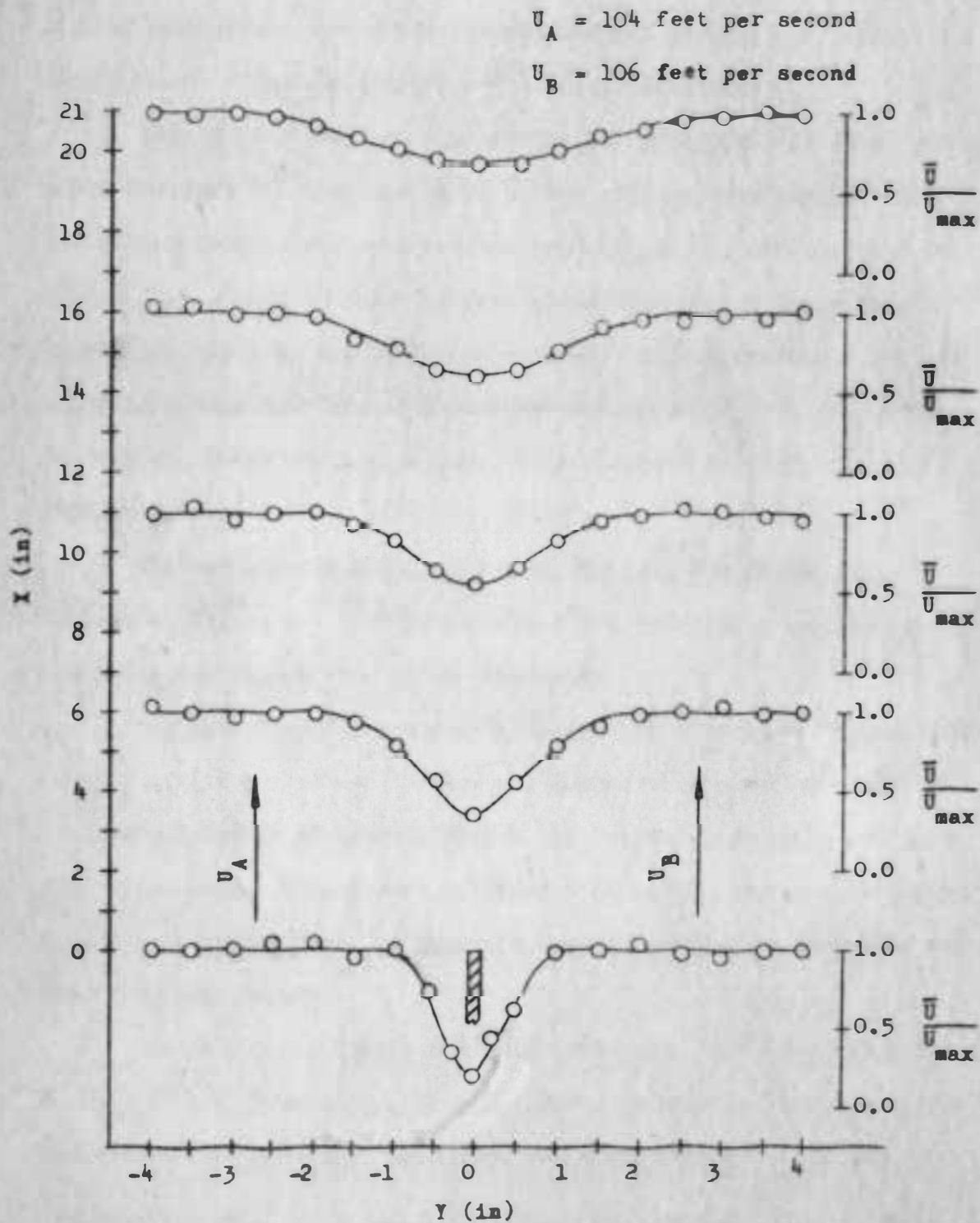


Figure IV. Velocity distribution for turbulent streams of equal velocities. (Ref. Table 1)

velocities, behind the splitter plate, recover faster for lower velocity streams. Based on the behaviour of wake velocities, and the boundary layer thickness law, it is reasonable to conclude that mixing boundaries for lower velocity streams spread faster than high velocity streams.

The mean velocity distribution, for the maximum free stream velocities of 195 feet per second and 49 feet per second in streams "B" and "A" respectively, was plotted in Figure VIII. The minimum velocity persists for a short distance downstream of flow, and then there is a smooth transition between two streams. Persistence of minimum velocity, for a short distance in the downstream direction, is due to a non-slip condition at the splitter plate. The non-slip condition disappears at the end of the splitter plate. Its effect does not disappear up to a distance of 6 inches from the end of the splitter plate. The mixing boundaries are thicker on the low velocity stream, which would be expected.

Temperature Distribution

Temperature measurements were made with stream "B" heated. However, it was discovered that there was also an approximately 8°F rise of temperature in stream "A." This was due to the excess pressure built behind the heating coils in stream "B." This excess pressure caused some of the heated air in stream "B" to be mixed with the cold air in stream "A." Even though the heating coil was located at a distance 2.5 feet downstream from the leading edge of the splitter

velocities, behind the splitter plate, recover faster for lower velocity streams. Based on the behaviour of wake velocities, and the boundary layer thickness law, it is reasonable to conclude that mixing boundaries for lower velocity streams spread faster than high velocity streams.

The mean velocity distribution, for the maximum free stream velocities of 195 feet per second and 49 feet per second in streams "B" and "A" respectively, was plotted in Figure VIII. The minimum velocity persists for a short distance downstream of flow, and then there is a smooth transition between two streams. Persistence of minimum velocity, for a short distance in the downstream direction, is due to a non-slip condition at the splitter plate. The non-slip condition disappears at the end of the splitter plate. Its effect does not disappear up to a distance of 6 inches from the end of the splitter plate. The mixing boundaries are thicker on the low velocity stream, which would be expected.

Temperature Distribution

Temperature measurements were made with stream "B" heated. However, it was discovered that there was also an approximately 8°F rise of temperature in stream "A." This was due to the excess pressure built behind the heating coils in stream "B." This excess pressure caused some of the heated air in stream "B" to be mixed with the cold air in stream "A." Even though the heating coil was located at a distance 2.5 feet downstream from the leading edge of the splitter

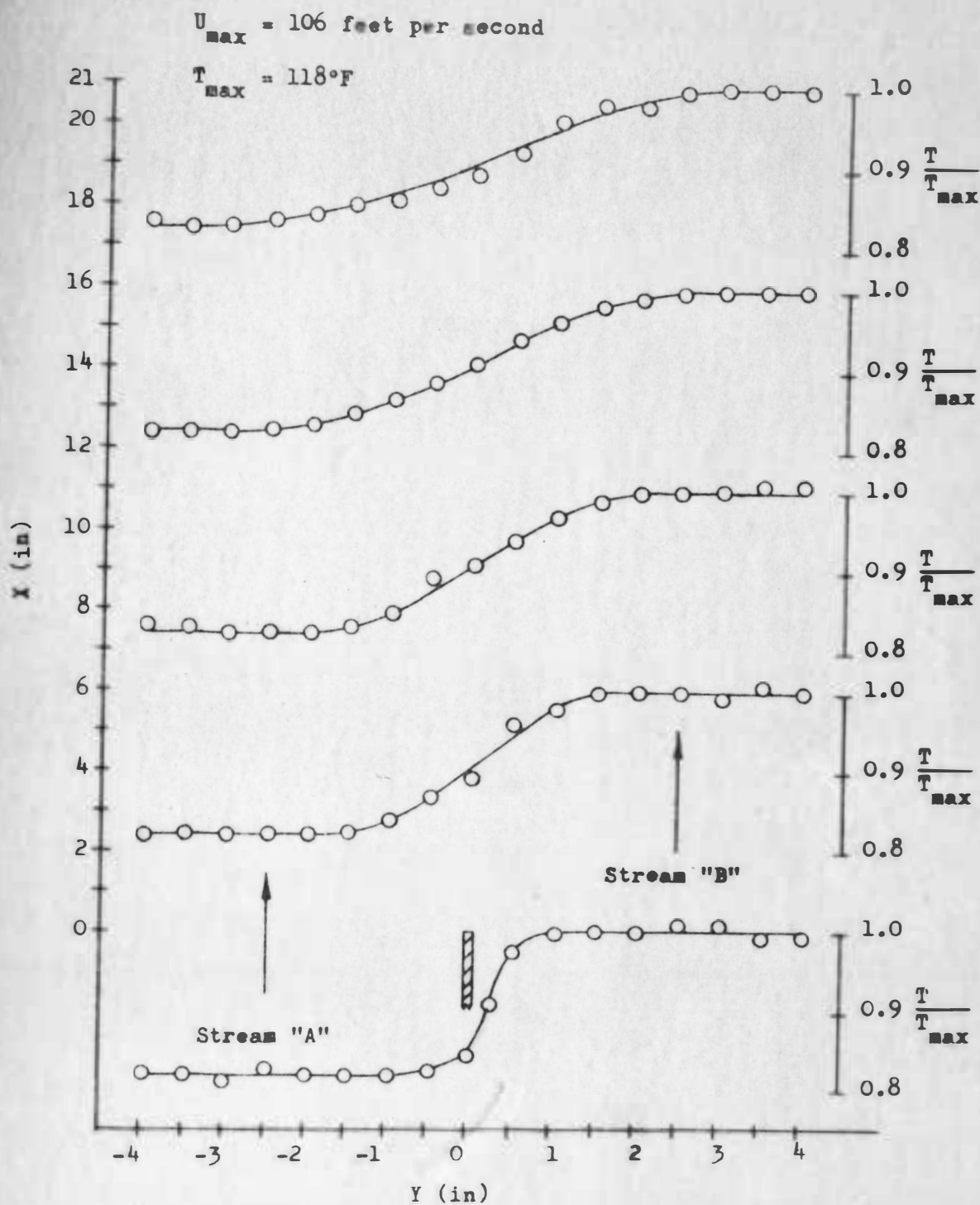


Figure V. Temperature distribution for turbulent streams of equal velocities and different densities. (Ref. Table 1)

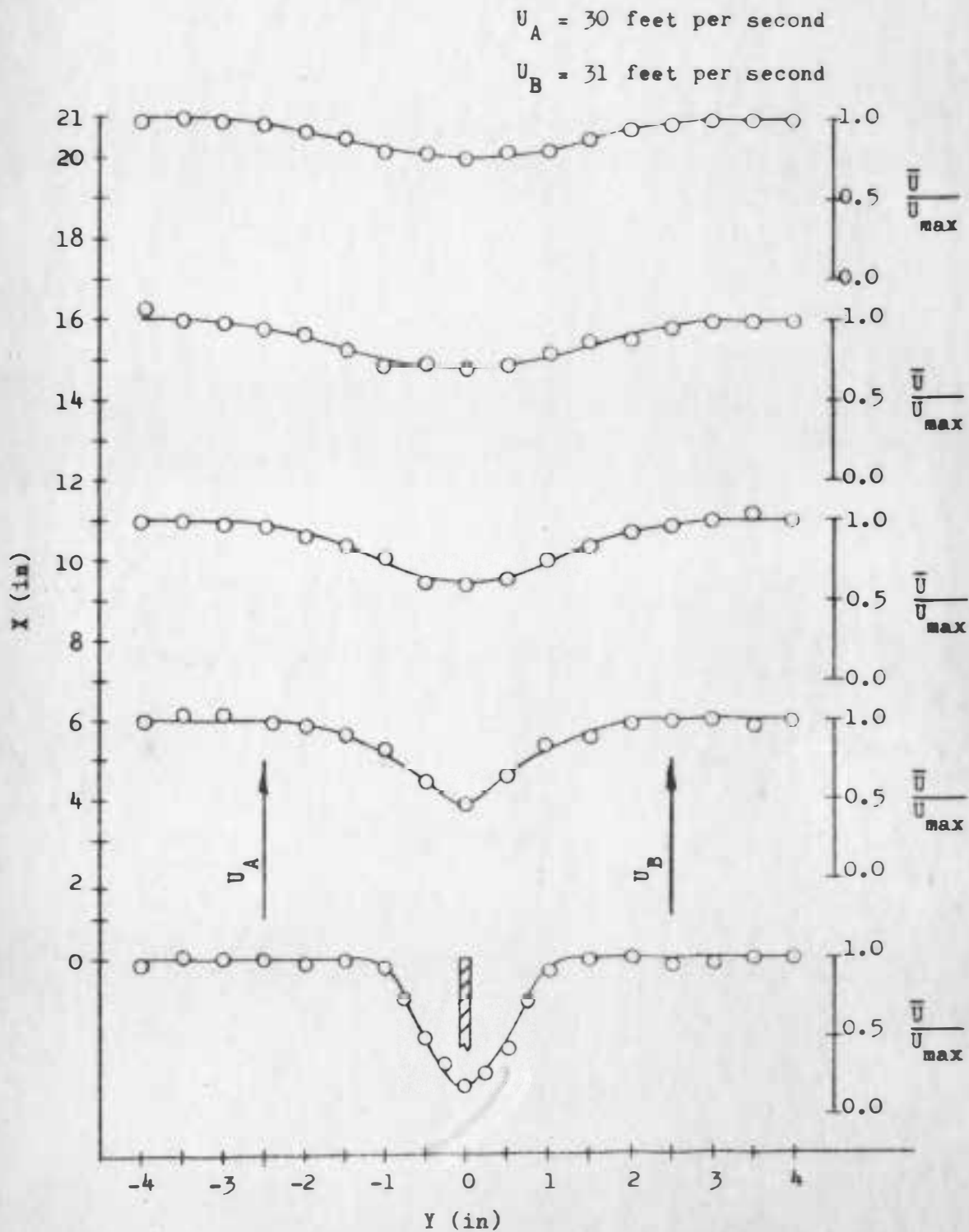


Figure VI. Velocity distribution for turbulent streams of equal velocities. (Ref. Table 2)

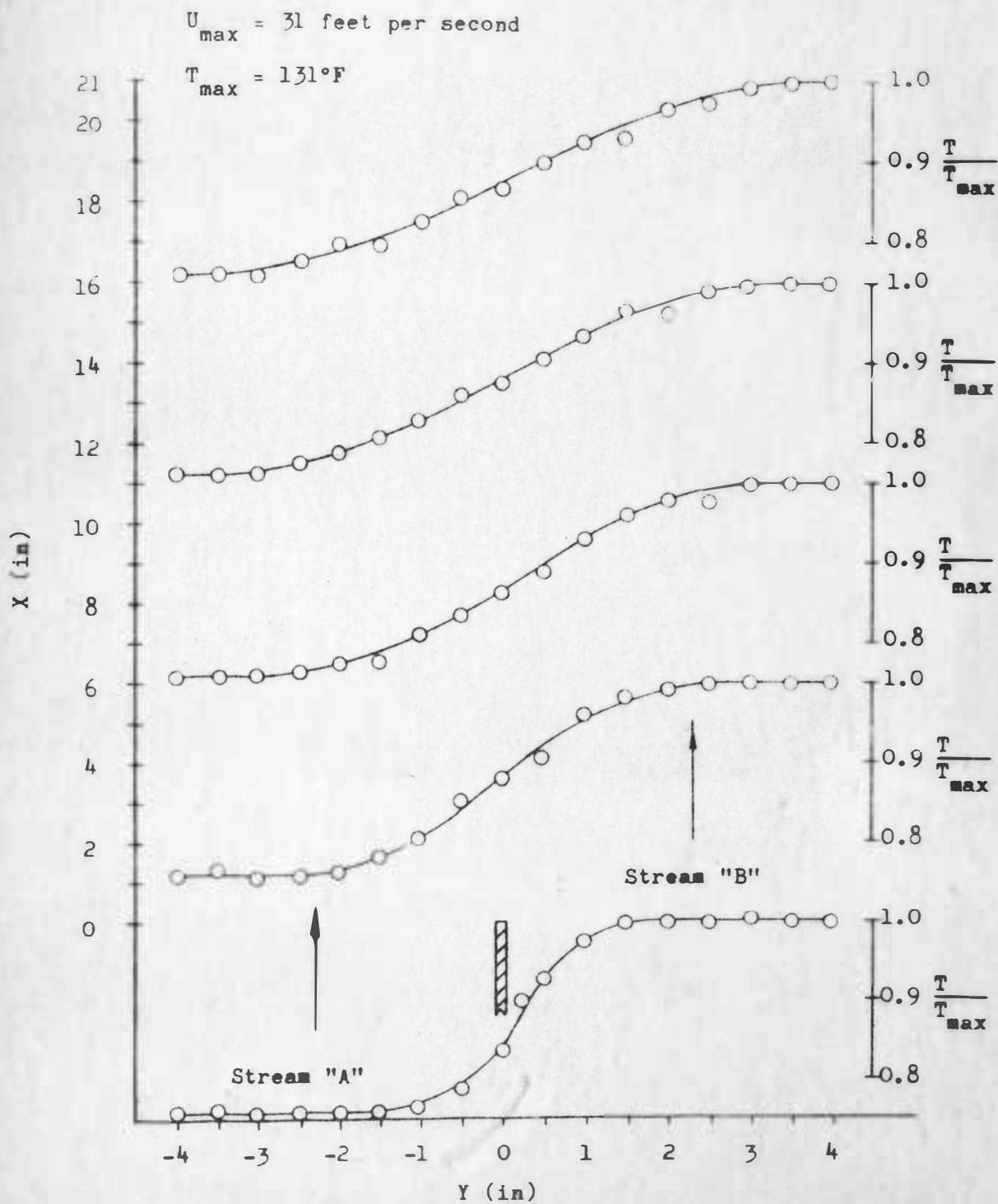


Figure VII. Temperature distribution for turbulent streams of equal velocities and different densities. (Ref. Table 2)

$U_A = 49$ feet per second

$U_B = 195$ feet per second

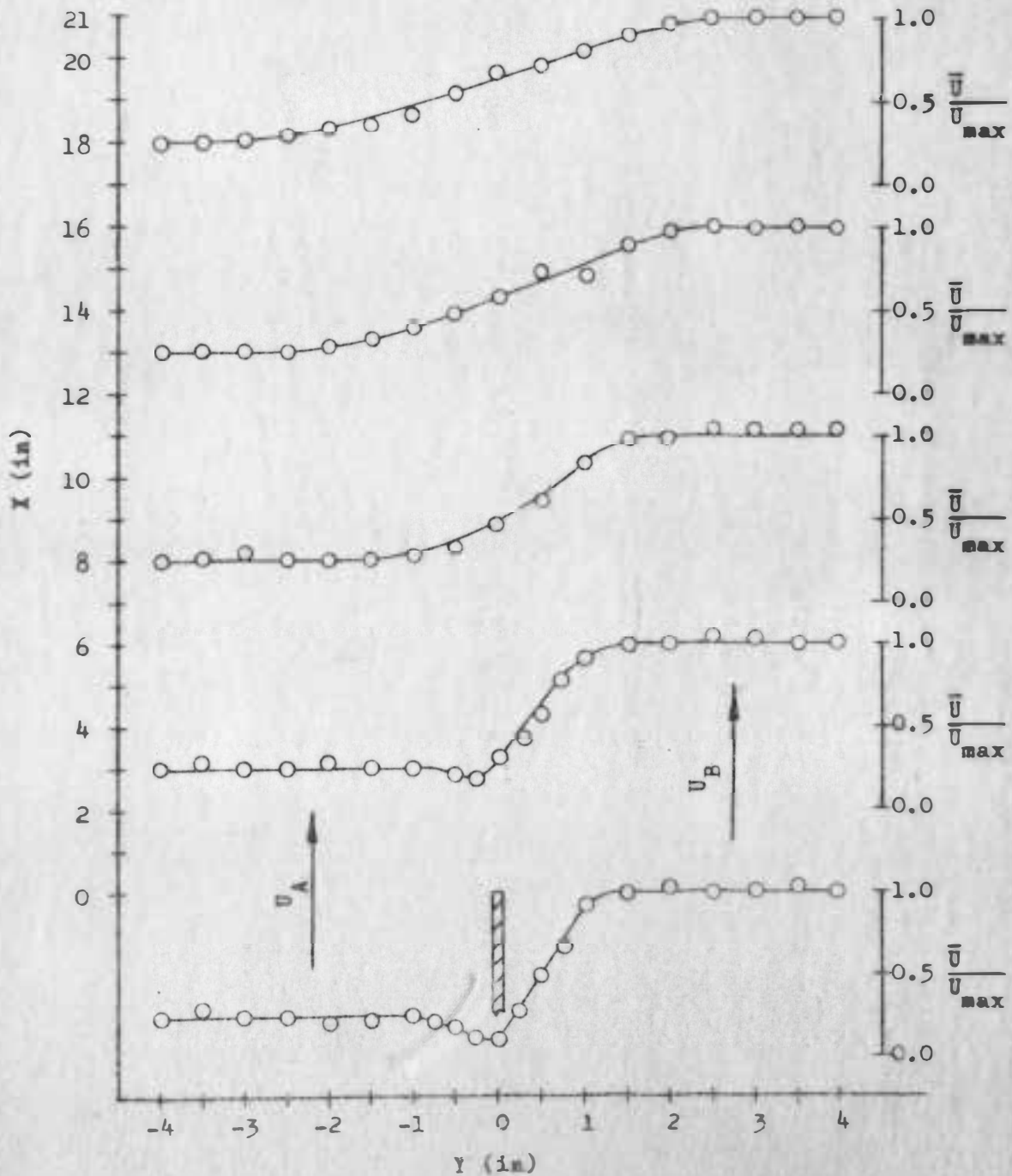


Figure VIII. Velocity distribution for turbulent streams of unequal velocities. (Ref. Table 3)

Momentum \square --- $U_{max} = 31$ feet per second
Momentum \circ --- $U_{max} = 106$ feet per second
Heat \triangle -- $U_{max} = 106$ feet per second
 $T_{max} = 118^{\circ}F$
Heat \triangle -- $U_{max} = 31$ feet per second
 $T_{max} = 131^{\circ}F$

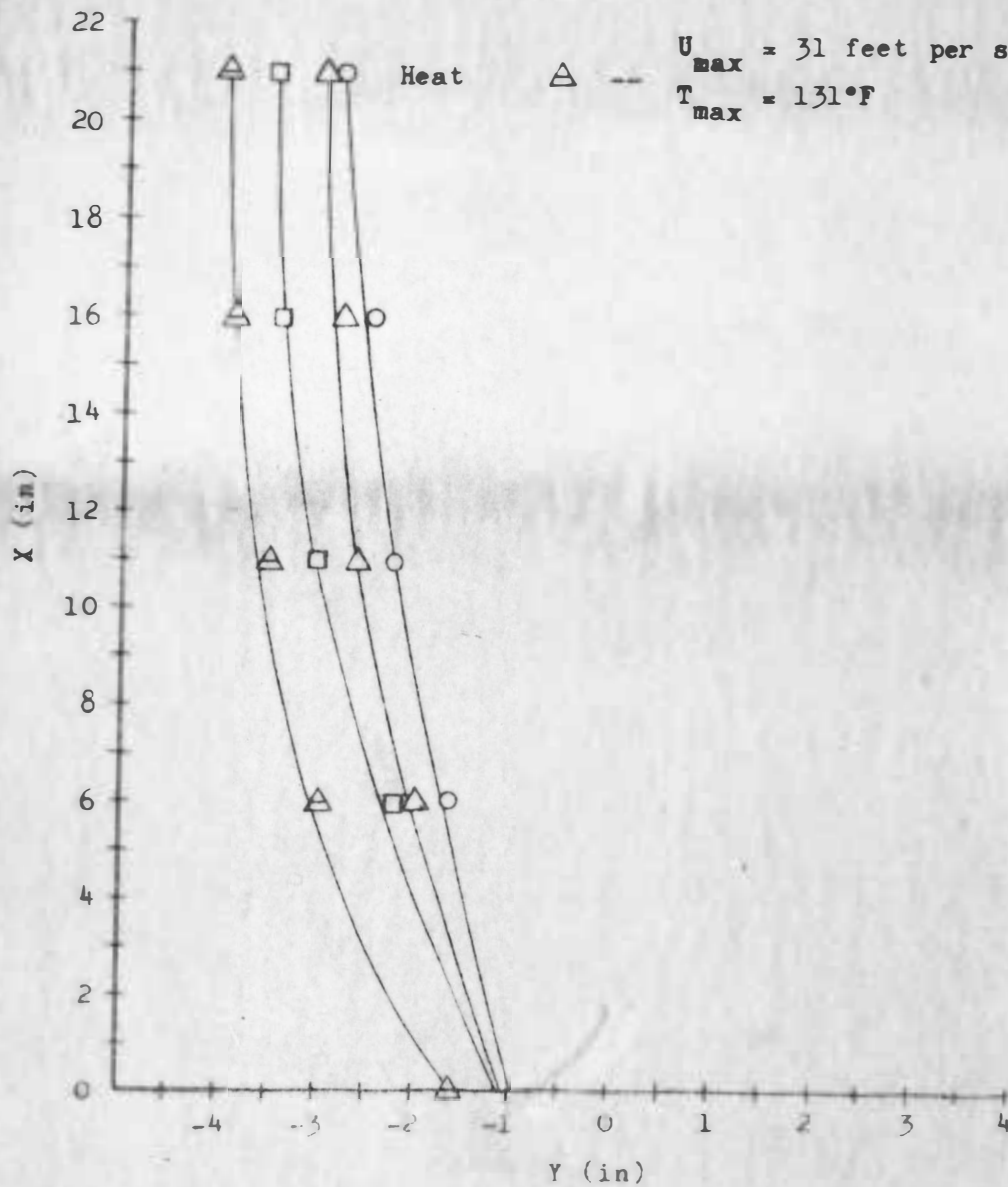


Figure IX. Mixing boundaries of heat and momentum

○ --- $U_{max} = 106$ feet per second
□ --- $U_{max} = 31$ feet per second

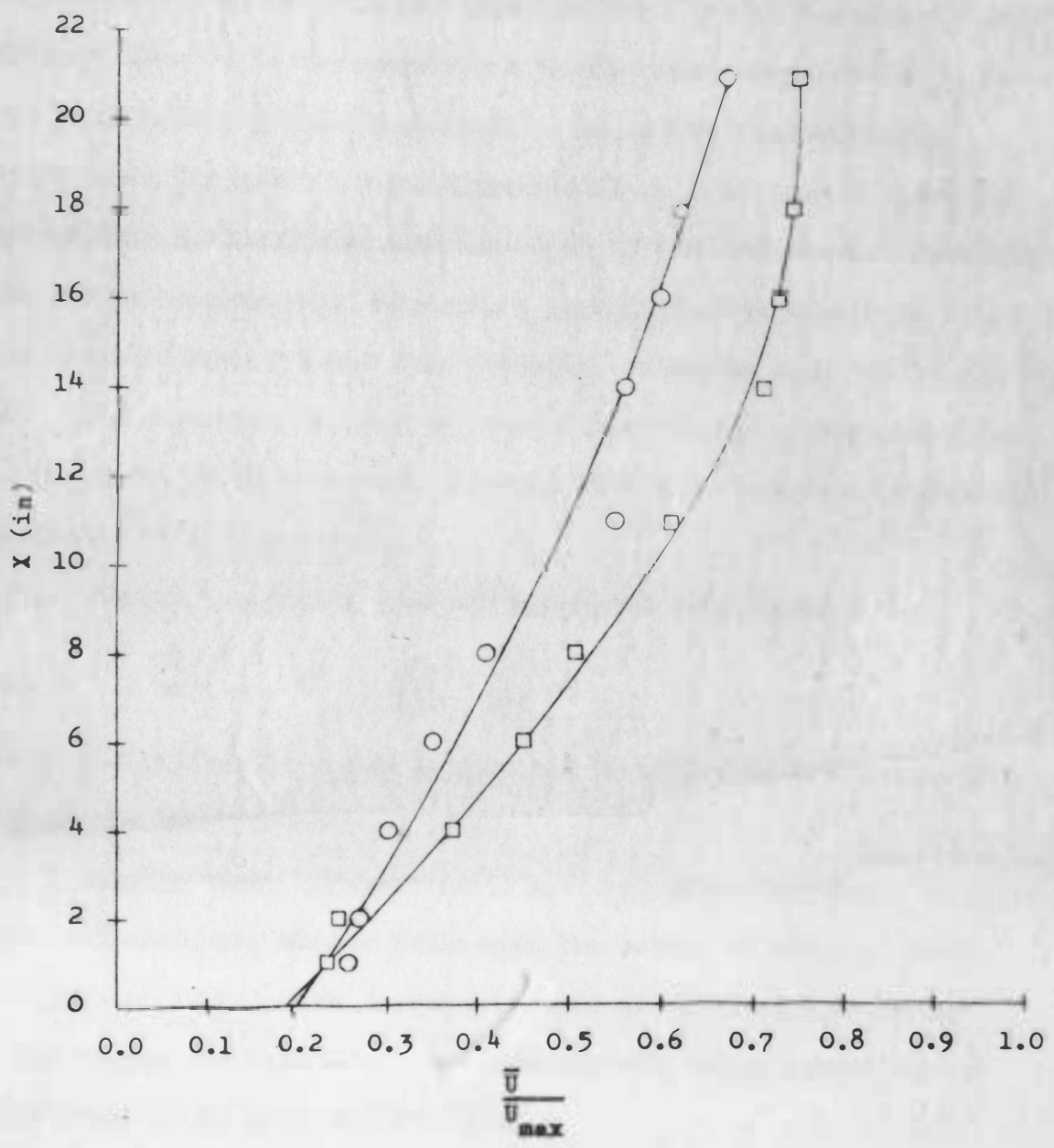


Figure X. Recovery of minimum velocity at the center of splitter plate

plate, this distance was not enough to overcome the effect of the back pressure.

Dimensionless parameter, T/T_{\max} was plotted against Y in Figures V and VII at different cross sections in the downstream direction of flow. T is the temperature in the mixing region and T_{\max} is the maximum free stream temperature. The mixing boundaries of temperature distribution were approximated at those points where the temperature in the mixing zone was equal to the free stream temperature. The mixing boundaries of temperature were plotted in Figure IX. Heat was found to spread faster than momentum, as can be seen from Figure IX. The reason for the wider spread of heat than of momentum can be explained by phenomenological theorems (Prandtl's momentum theorem and Taylor's vorticity theorem).

Prandtl's momentum theorem¹⁹ is stated as follows:

$$(13) \quad \overline{u'v'} = L^2 \rho \left| \frac{d\bar{u}}{dY} \right| \frac{d\bar{u}}{dY}$$

Where L is called the mixing length, and is analogous to the mean free path in the kinetic theory of gases.

Kinetic theory of gases deals with the molecular motion in gases, while mixing length theorem deals with the motion of lumps of fluid. The lumps of fluid travel in the direction of flow and also travel in the transverse direction. The high velocity lumps impart some of their momentum to lower velocity lumps.

¹⁹ Schlichting, op. cit., p. 386.

According to the momentum transfer theorem, momentum and heat are transferred by the same process. Experiments performed on the spread of round heated jets²⁰ and on the wakes behind heated cylinders,²¹ show that the spread of heat is faster than the spread of momentum.

The mechanism, by which heat and momentum are transferred, is evidently not identical. According to a new line of thought, heat is transferred by the circulation of fluid particles in the turbulent fluid. The circulation is so-called vorticity. Taylor's vorticity theorem²² can be stated as follows:

$$(14) \quad \overline{u'v'} = \frac{1}{2} L_w^2 \rho \left| \frac{d\bar{U}}{dY} \right| \frac{d\bar{U}}{dY}$$

where L_w is the mixing length. Comparing Taylor's vorticity theorem and Prandtl's momentum theorem, L_w is larger by a factor of $\sqrt{2}$, than L . The longer mixing length for Taylor's vorticity theorem gives a wider spread of heat than momentum.

The correlation between temperature and velocity fluctuations was measured in a one inch round turbulent heated jet by Corrsin and

²⁰Corrsin and Uberio, op. cit., p. 30.

²¹A. A. Townsend, The Fully Developed Wake of a Circular Cylinder, Australian Journal of Scientific Research, Series A, Vol. 2, pp. 452-468, 1949.

²²Schlichting, op. cit., p. 391.

Uberio.²³ They measured the following correlation coefficients for the case of turbulent flow:

$$(15) \quad R_{T'V'} = \frac{\overline{T'V'}}{\sqrt{\overline{T'^2}} \sqrt{\overline{V'^2}}}$$

$$(16) \quad R_{U'V'} = \frac{\overline{U'V'}}{\sqrt{\overline{U'^2}} \sqrt{\overline{V'^2}}}$$

$R_{T'V'}$ was found to be greater than $R_{U'V'}$, which was anticipated since the rate of heat transfer is known to be greater than the rate of momentum transfer.

Intensity of Turbulence

Longitudinal intensity of turbulence $\sqrt{\overline{U'^2}}/\bar{U}$ was measured with a hot-wire anemometer and a random signal voltmeter. Maximum free stream velocities in streams "B" and "A" were 28 feet per second and 26 feet per second respectively. Intensity of turbulence was plotted against Y in Figure XI at X = 0, 6, 11, 16 and 21 inches. In the potential flow at X = 0, the intensity of turbulence remains constant. Close to the mixing boundaries, the intensity of turbulence starts to increase, and reaches its maximum point at the center of the separating plate. The turbulence mixing boundaries were approximated at those points where intensity of turbulence was at its minimum. Further outward, the intensity of turbulence remained constant. Further

²³Corrsin and Uberio, op. cit., p. 15.

downstream of $X = 0$, the mixing boundaries of momentum and the mixing boundaries of turbulence spread laterally. On comparing Figures XI and IV, the mixing boundaries of momentum and the mixing boundaries of turbulence follow the same pattern.

The intensity of turbulence for a maximum free stream velocity of 130 feet per second and 127 feet per second in streams "B" and "A" respectively, was plotted against Y in Figure XII. The mixing boundaries of turbulence seem to spread faster for low velocity streams. This is expected from the fact that low velocity streams spread faster than the high velocity streams.

The intensity of turbulence at the center of the separating plate was plotted in Figure XIII. At $X = 0$, the intensity of turbulence is at its maximum, and further downstream there is a decay of intensity of turbulence. As a result, the turbulent velocities are transferred into mean velocities. Mean velocities are at their minimum at $X = 0$, and further downstream they are in the process of recovery.

As can be seen from Figure XIII, the intensity of turbulence is higher for low velocity streams. Wattendorf and Kuethe,²⁴ in 1934, measured longitudinal turbulence in air flowing through a pipe at various Reynold's numbers, and found the intensity of turbulence

²⁴ F. L. Wattendorf and A. M. Kuethe, Investigations of Turbulent Flow by Means of the Hot-Wire Anemometer, Journal of Applied Physics, Vol. 5, pp. 153-164, 1934.

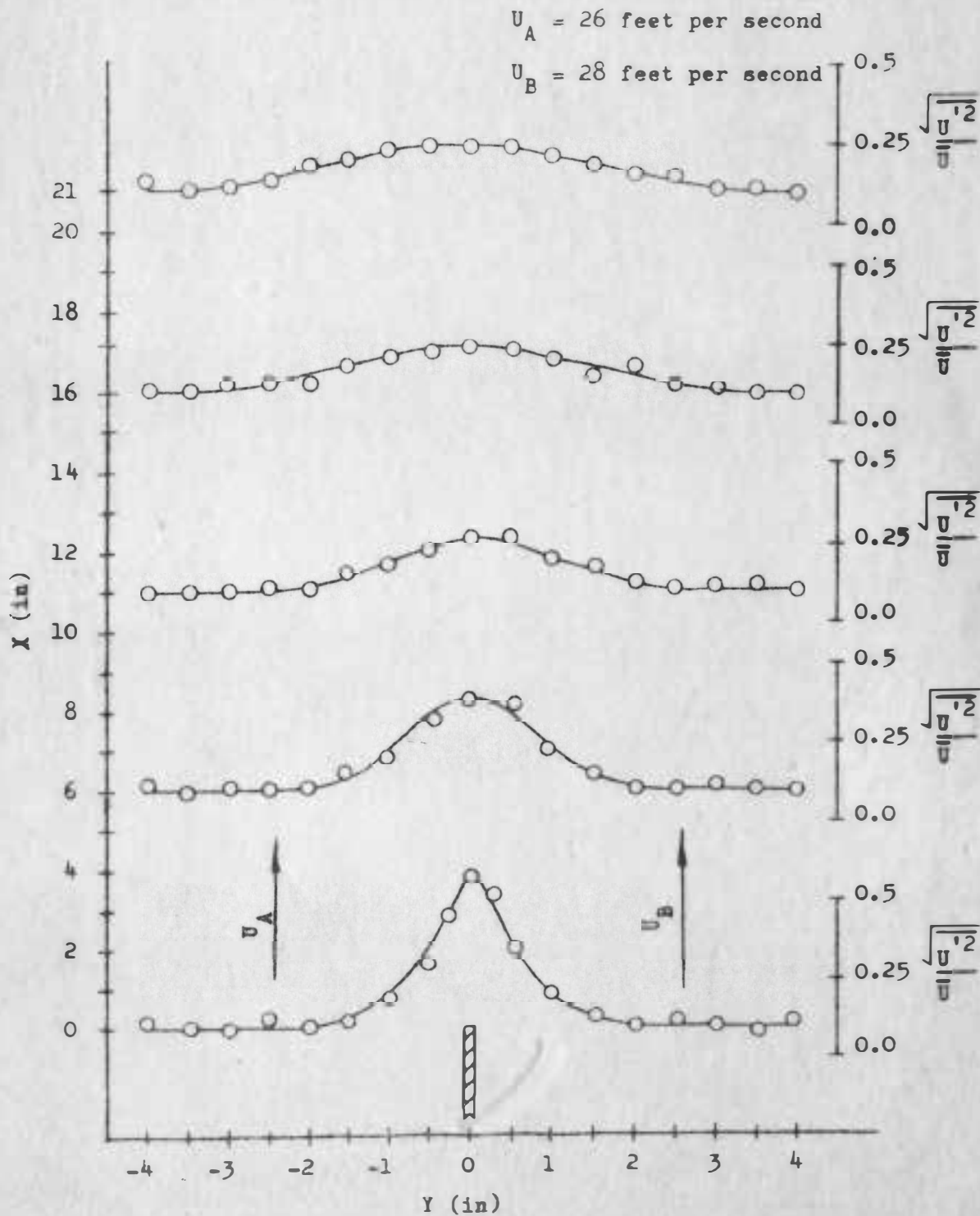


Figure XI. Intensity of turbulence for streams of equal velocities. (Ref. Table 4)

$U_A = 127$ feet per second

$U_B = 130$ feet per second

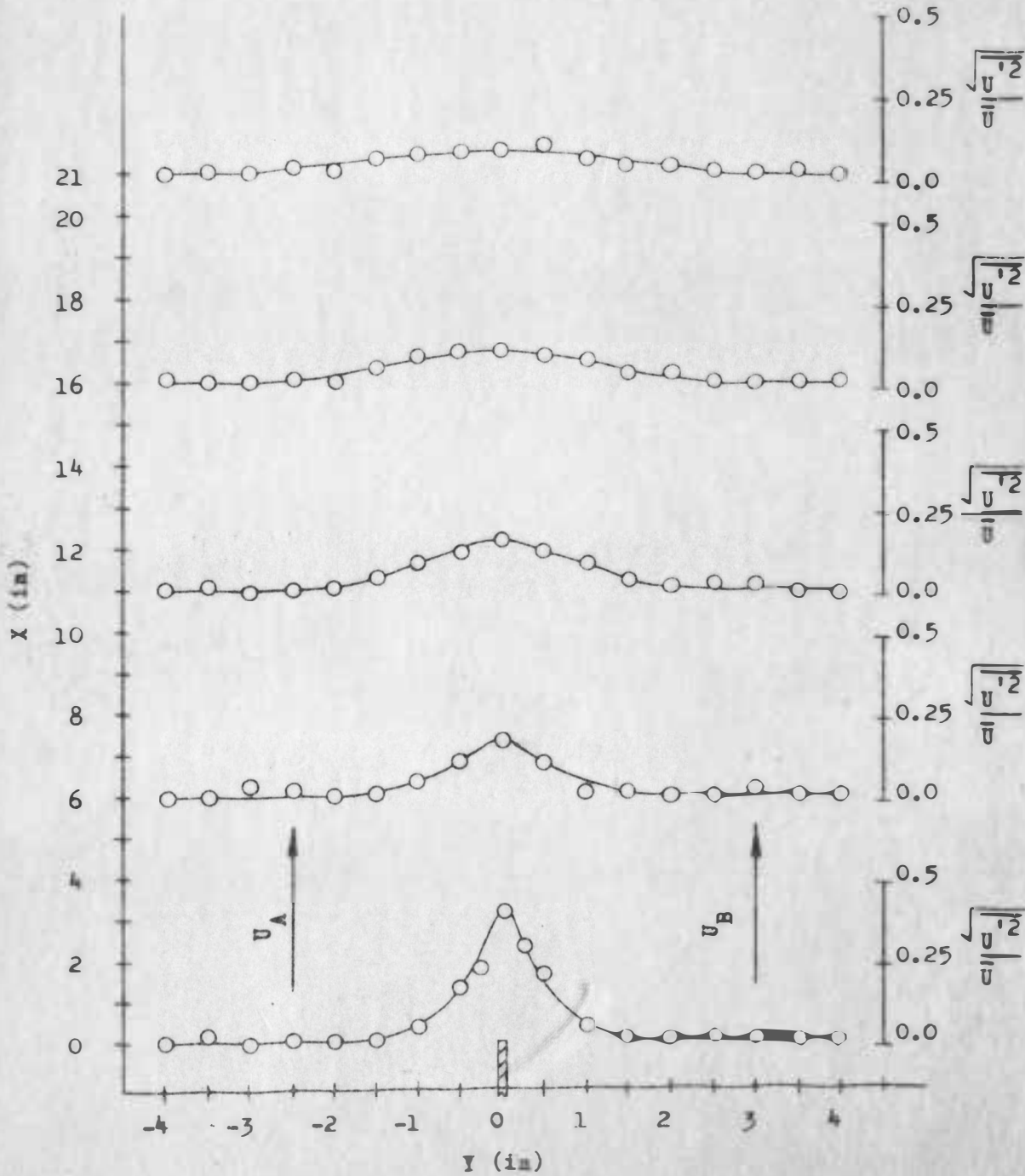


Figure III. Intensity of turbulence for streams of equal velocities

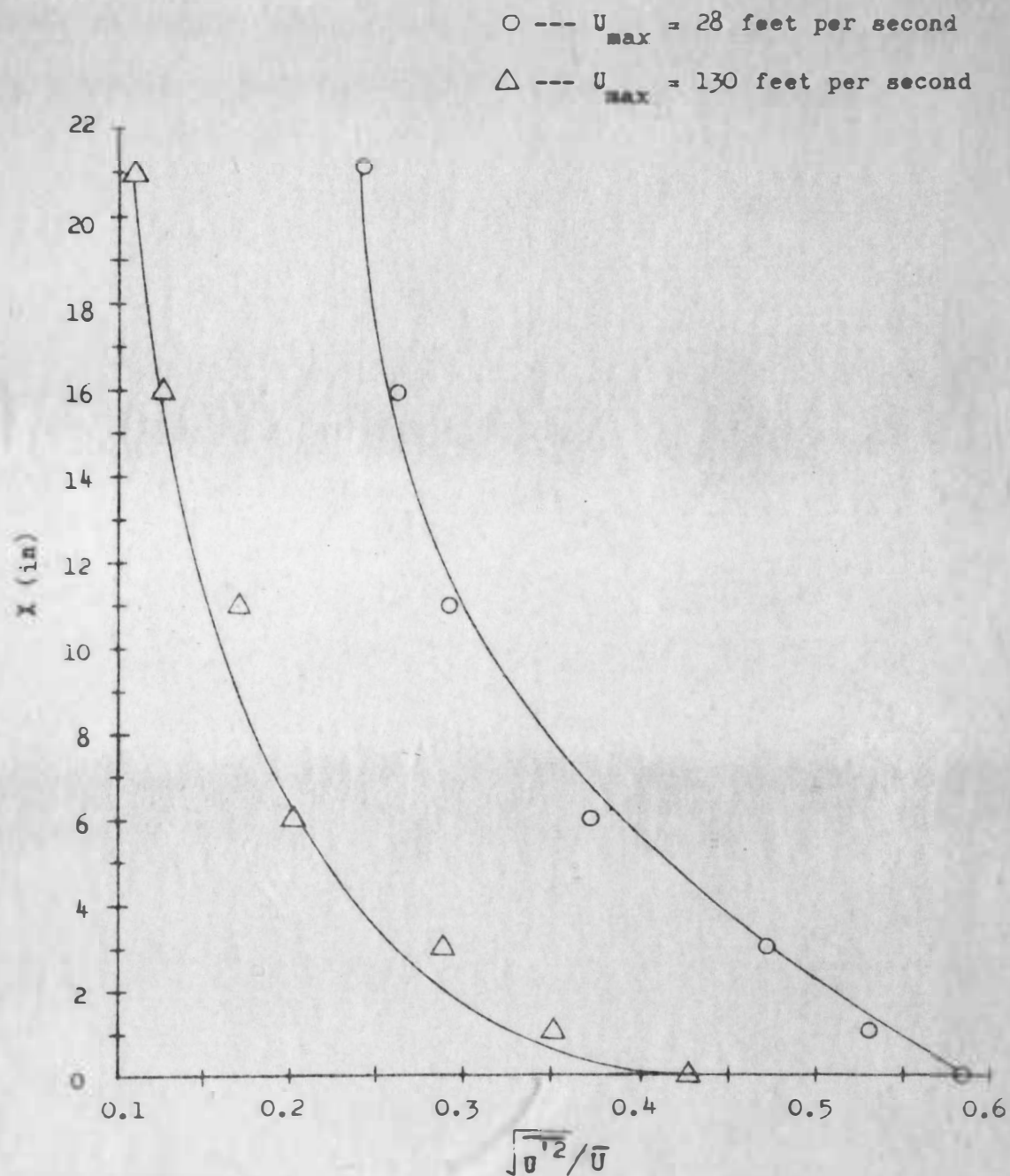


Figure XIII. Dissipation of intensity of turbulence at the center of splitter plate

higher for low Reynold's numbers. Laufer,²⁵ in 1950, conducted experiments on a fully developed turbulent flow in a channel, and found the intensity of turbulence higher for low Reynold's numbers.

²⁵J. Laufer, Some Recent Measurements in a Two-Dimensional Turbulent Channel, Journal of the Aeronautical Sciences, Vol. 17, pp. 277-287, 1950.

CHAPTER VII

CONCLUSIONS AND RECOMMENDATIONS

Summary of Results

1. The design modifications in the wind tunnel introduced the following flow characteristics:
 - a. The velocity profiles at the test section were flat.
 - b. The intensity of turbulence was reduced to about 3.0%.
 - c. The boundary layer at the start of the mixing zone was widened.

In view of the above results, the wind tunnel is ready for more qualitative and quantitative experiments.

2. The mixing boundaries were not a straight line function of the downstream distance, but were curved.
3. The mixing boundaries of lower velocity streams were found to spread faster than high velocity streams.
4. The spread of heat was found to be greater than the spread of momentum.
5. The mixing boundaries of momentum, and the mixing boundaries of turbulence follow the same pattern.
6. The intensity of turbulence was higher for low velocity streams.

Recommendations

It is highly recommended that the work on this project should continue beyond the present investigation. The extension of the present investigation may include the following:

1. A random signal correlator and a sum-difference control unit might be purchased from the Flow Corporation. These instruments with the combination of a random signal voltmeter could be used to measure the longitudinal and the transverse components of turbulence, the correlation between longitudinal and transverse components, and the correlation between two longitudinal components. As to the author's knowledge, these parameters had not been measured previously in the wind tunnel for the particular case of mixing of two turbulent streams. Even, if there might be a certain amount of duplication, the importance of this project should not be minimized. A certain amount of duplication is rather a necessary and an important part of applied research.
2. The temperature difference between two streams might be increased. This could be accomplished by either increasing the surface area of the existing steam heating coil or by supplying the steam at an increased pressure. Further, there could be a possibility of installing an electric heating coil in series with the existing steam heating coils.

3. As mentioned earlier on page 26, there was an 8°F rise of temperature in stream "A." This was due to a back-pressure buildup behind the heating coil in stream "B." This might be remedied by installing a restriction in stream "A" equal to the amount of restriction caused by heating coil in stream "B." Thus, the temperature difference between two streams would increase by 16°F .
4. Further investigation might include the application of hot-wire equipment for measurements of temperature and temperature fluctuations.

LITERATURE CITED

1. Abramovich, G. N., The Theory of a Free Jet of a Compressible Gas. N.A.C.A., TM No. 1058. March, 1944.
2. Bulletin No. 37D, Model HWB3 Hot-Wire Anemometer Theory and Instructions. p. 33. Flow Corporation, 205 Sixth Street, Cambridge 42, Massachusetts.
3. Childs, M. E., and Associates, Two-Dimensional Turbulent Mixing Between Parallel Jets Considering Effects of Initial Boundary Layer. The University of Washington, Department of Mechanical Engineering. October 16, 1962.
4. Corrsin, S., Investigation of Flow in an Axially Symmetrical Heated Jet of Air. N.A.C.A., ACR No. 3L23, W-94. 1943.
5. Corrsin, S., and M. S. Uberio, Further Experiments on the Flow and Heat Transfer in a Heated Turbulent Air Jet. N.A.C.A., TN No. 1865. 1949.
6. Hottel, H. C., and A. Kalitinsky, Temperature Measurements in High Velocity Air Streams. Journal of Applied Mechanics. Vol. 67. pp. A25-A32. 1945.
7. Iverson, R. A., The Design of an Apparatus for Investigating Turbulent Mixing of Two Parallel Air Streams and Analysis of Half-Jet Phenomena. M.S. Thesis, South Dakota State University. 1964.
8. Kuethe, A. M., Investigations of Turbulent Mixing Region Formed by Jets. Journal of Applied Mechanics. Vol. 2. pp. A87-A95. 1935.
9. Laufer, J. Some Recent Measurements in a Two-Dimensional Turbulent Channel. Journal of the Aeronautical Sciences. Vol. 17. pp. 277-287. 1950.
10. Liepmann, H. W., and J. Laufer, Investigations of Free Turbulent Mixing. N.A.C.A., TN No. 1257. 1947.
11. Schlichting, H. Boundary Layer Theory. McGraw-Hill Book Company. New York, 1955.
12. Tollmien, W. Calculation of Turbulent Expansion Processes. N.A.C.A., TM No. 1085. 1945.

13. Torda, T. P., and H. S. Stillwell, Analytical and Experimental Investigations of Incompressible and Compressible Mixing of Streams and Jets. WADC Technical Report 55347. 1956.
14. Townsend, A. A., The Fully Developed Wake of a Circular Cylinder. Austrian Journal of Scientific Research. Series A. Vol. 2. pp. 452-468. 1949.
15. Wattendorf, F. L., and A. M. Kuethe, Investigations of Turbulent Flow by Means of the Hot-Wire Anemometer. Journal of Applied Physics. Vol. 5. pp. 153-164. 1934.

APPENDIX A

For the accurate measurements of mean velocities, the hot-wire probe was calibrated. The calibration curve of I^2 versus $(P_{\text{abs}} \bar{U})^{1/2}$ is shown in Figure XIV. The velocities and static pressures were measured with a conventional pitot tube and inclined manometers.

For the hot-wire anemometer, a resistance ratio of 1.2 was selected and became a standard for subsequent measurements. The galvanometer needle was more stable at this resistance ratio.

As can be seen from Figure XIV, the calibration curve is a straight line. From this curve, the following equation was derived:

$$\bar{U} = \frac{(I^2 - 3750)^2}{34276.87 P_{\text{abs}}}$$

This equation is in a very convenient form to compile a computer program.

Resistance ratio = 1.2

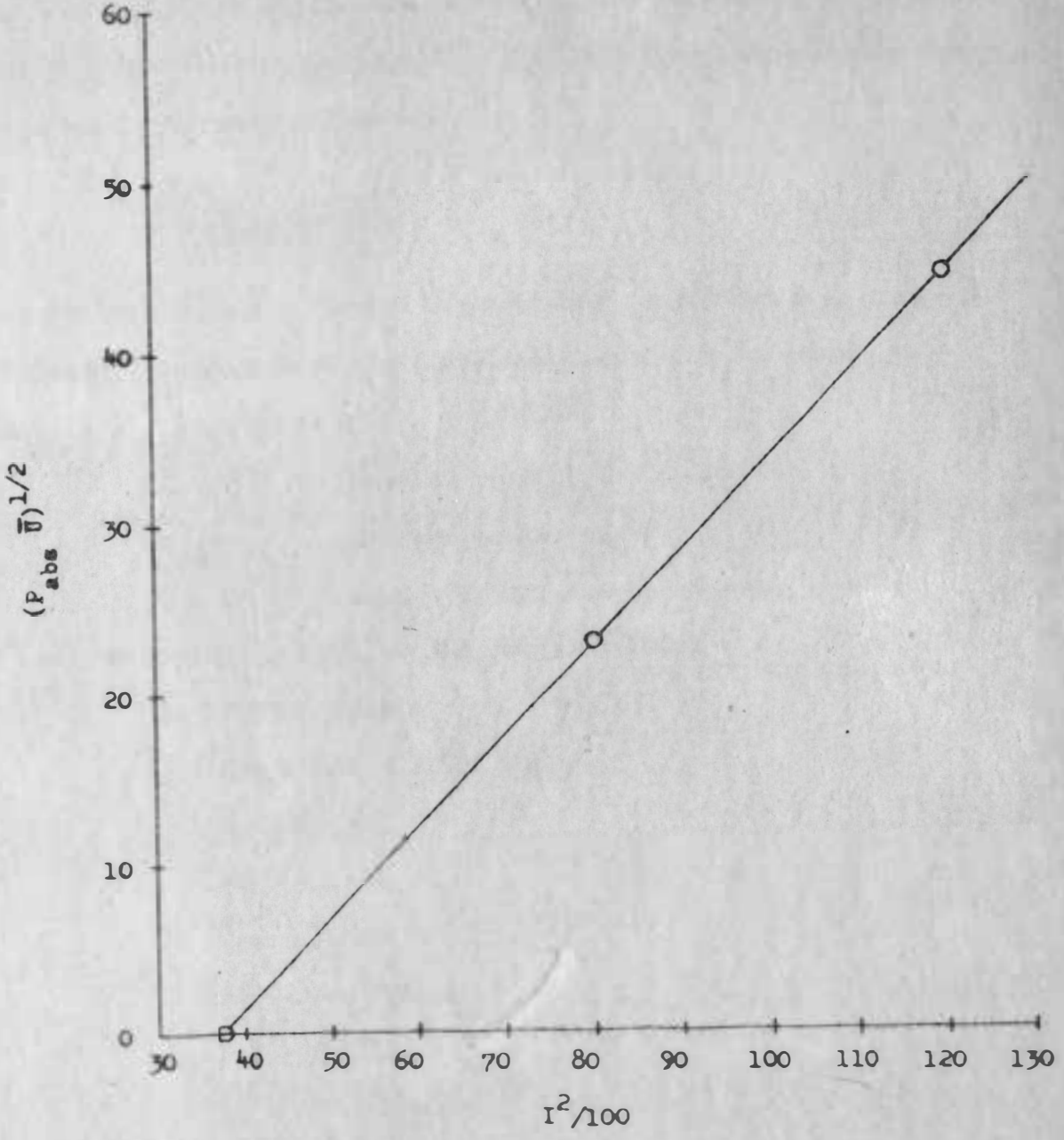


Figure XIV. Hot-wire probe calibration curve

APPENDIX B

A 1620 digital computer was available for the computation of mean velocities and intensities of turbulence. A Fortran language was used to write the computer program. The following equation was used to calculate the mean velocities:

$$\bar{U} = \frac{(I^2 - 3750)^2}{34276.87 P_{\text{abs}}}$$

To avoid any confusion between floating-point variables and fixed-point variables, the symbols in the above equation had to be replaced as follows:

I = CI hot-wire current, milliampères
 P_{abs} = P absolute pressure, psia
 \bar{U} = U mean velocity, feet per second

The Fortran program was written as follows:

```

65  FORMAT (F7.3)
40  FORMAT (F8.3, F8.3, F8.3)
1   READ 65, P
    READ 65, CI
    CU = CI * CI
    CO = CU - 3750.0
    CA = CO * CO
    CF = P * 34276.87
    U = CA/CF

```

PRINT 40, U, P, CI

GO TO 1

END

APPENDIX C

The following equation was used to calculate the intensity of turbulence:

$$\frac{\sqrt{U'^2}}{\bar{U}} = \frac{4 I_C}{I \left[1 - \left(\frac{I_0}{I} \right)^2 \right]} \sqrt{\frac{M_1^2 - M_2^2}{M_3^2 - M_1^2}}$$

The symbols in the above equation were replaced as follows:

$I_C = VIC$ square wave current, milliamperes

$I = VI$ hot-wire current, milliamperes

$I_0 = VIO$ hot-wire current at zero velocity, milliamperes

$M_1 = VM1$ random signal voltmeter reading, hot-wire heated, millivolts

$M_2 = VM2$ random signal voltmeter reading, hot-wire unheated, millivolts

$M_3 = VM3$ random signal voltmeter reading, hot-wire heated and square wave superimposed, millivolts

$$\frac{\sqrt{U'^2}}{\bar{U}} = A \quad \text{intensity of turbulence}$$

The Fortran program was written as follows:

40 FORMAT (F8.6, 6F10.4)

LE = CDSF (9.0)

```
2 ACE = RCDF (1.0)
VIC = GETF (1042.2)
VI = GETF (1083.1)
VIO = GETF (1123.1)
VM1 = GETF (1174.1)
VM2 = GETF (1212.1)
VM3 = GETF (1264.1)
B = 4.0 * VIC
C = VIO/VI
D = C * C
DE = 1.0 - D
DI = VI * DE
VM4 = (VM1 * VM1) - (VM2 * VM2)
VM5 = (VM3 * VM3) - (VM1 * VM1)
VM = VM4/VM5
VMS = SQRTF (VM)
DS = B/DI
A = DS * VMS
PRINT 40, A, VIC, VI, VIO, VM1, VM2, VM3
GO TO 2
END
```

Table 1. Velocity and Temperature Distribution for Turbulent Streams of Equal Velocities. (Ref. Figures IV and V)

$$P_{abs} = 14.407 \text{ psia}$$

X (in)	Y (in)									
	-4	-3	-2	-1	0	1	2	3	4	
0	I	104.50	104.50	104.75	104.50	83.50	104.75	105.25	104.25	104.75
	\bar{U}	104.1	104.1	105.6	104.1	21.02	105.6	108.7	102.6	105.6
	T	96.6	95.5	96.6	96.6	98.2	118.1	118.1	118.8	116.8
6	I	104.75	104.00	104.50	101.25	88.50	101.25	104.75	105.50	104.75
	\bar{U}	105.6	101.1	104.1	85.6	33.7	85.6	105.6	110.3	105.6
	T	96.5	96.7	96.6	98.6	105.0	112.7	118.2	116.6	118.0
11	I	104.5	104.0	104.50	102.0	95.50	95.50	104.75	105.25	104.25
	\bar{U}	104.1	101.1	104.1	89.7	58.4	58.4	105.6	108.7	102.6
	T	97.9	96.6	97.0	99.8	106.7	114.5	118.1	118.5	119.0
15	I	104.75	104.00	104.00	100.00	97.00	100.00	104.25	104.75	105.25
	\bar{U}	105.6	101.1	101.1	79.1	64.8	79.1	102.6	105.6	108.7
	T	96.6	96.6	97.8	101.4	106.7	113.1	116.8	118.0	118.2
21	I	104.50	104.50	103.00	100.00	99.75	100.00	103.00	104.75	104.75
	\bar{U}	104.1	104.1	95.3	79.1	77.8	79.1	95.3	105.6	105.6
	T	97.9	96.5	99.1	100.8	105.0	112.7	115.0	118.0	118.0

APPENDIX D

Table 2. Velocity and Temperature Distribution for Turbulent Streams of Equal Velocities. (Ref. Figures VI and VII)

$$P_{\text{abs}} = 14.615 \text{ psia}$$

X (in)		Y (in)								
		-4	-3	-2	-1	0	1	2	3	4
0	I	87.50	87.50	87.25	87.25	75.5	87.00	87.75	87.25	87.75
	\bar{U}	29.78	30.46	29.78	29.78	7.60	29.11	31.14	29.78	31.14
	T	99.2	99.2	99.2	100.3	110.0	127.0	131.0	131.9	130.6
6	I	87.50	88.00	87.25	85.25	79.50	86.00	87.50	87.75	87.75
	\bar{U}	29.78	31.84	29.78	24.70	13.18	26.53	30.46	31.14	31.14
	T	99.2	89.9	100.4	105.2	115.2	125.8	129.5	131.1	131.1
11	I	87.50	87.50	86.50	84.75	82.75	84.75	86.75	87.75	87.50
	\bar{U}	30.46	30.46	27.81	23.51	19.15	23.51	28.45	31.14	30.46
	T	99.1	99.1	101.4	105.9	112.7	121.6	128.2	130.8	131.1
16	I	88.0	87.50	86.50	84.50	84.25	85.25	85.50	87.75	87.75
	\bar{U}	31.84	29.78	27.81	22.94	22.38	24.70	25.30	31.14	31.14
	T	99.1	99.1	103.3	108.8	114.1	122.1	122.1	130.7	131.0
21	I	87.00	87.50	86.50	85.00	84.50	85.25	86.50	87.75	87.75
	\bar{U}	29.11	29.78	27.81	24.1	22.94	24.70	27.81	31.14	31.14
	T	99.0	99.1	104.8	108.1	113.8	120.6	126.3	129.7	131.1

Table 3. Velocity and Temperature Distribution for Turbulent Streams of Unequal Velocities. (Ref. Figure VIII)

$P_{abs} = 13.905$ psia

X (in)		Y (in)								
		-4	-3	-2	-1	0	1	2	3	4
0	I	92.50	92.50	90.00	92.00	83.25	114.0	116.25	115.75	115.75
	\bar{U}	48.46	48.46	39.70	46.62	21.22	179.36	200.02	195.30	195.30
6	I	92.50	92.50	93.25	92.50	95.00	174.82	115.75	116.25	115.75
	\bar{U}	48.46	48.46	51.36	48.46	58.38	113.50	195.30	200.02	195.30
11	I	92.50	95.00	92.50	93.75	101.50	166.42	115.75	116.25	116.25
	\bar{U}	48.46	58.38	48.46	53.28	90.07	112.50	195.30	200.02	200.02
16	I	93.00	92.50	93.75	99.50	105.00	108.75	115.25	115.75	115.75
	\bar{U}	50.35	48.46	53.28	79.36	111.04	137.20	190.65	195.30	195.30
21	I	92.50	93.25	97.25	101.25	108.0	112.25	115.25	115.75	115.75
	\bar{U}	48.46	51.36	68.35	88.68	131.40	164.33	190.65	195.30	195.30

Table 4. Intensity of Turbulence for Streams of Equal Velocities
(Ref. Figure XI)

$$P_{abs} = 14.622, \quad I_o = 63.75, \quad I_C = 6.40, \quad M_2 = 2.25, \quad A = \sqrt{U'^2/\bar{U}}$$

X (in)		Y (in)								
		-4	-3	-2	-1	0	1	2	3	4
0	I	86.50	86.50	86.25	86.25	73.75	86.00	86.75	86.25	86.75
	M ₁	76.00	70.0	70.0	135.0	185.0	135.0	74.00	74.00	80.00
	M ₃	468.0	470.0	465.0	475.0	474.0	460.0	470.0	470.0	480.0
	\bar{U}	27.79	27.79	27.15	27.15	5.7	26.52	28.44	27.15	28.44
	A	.106	.097	.099	.193	.582	.202	.102	.104	.108
6	I	86.50	87.00	86.75	84.25	78.50	85.0	86.50	86.75	86.75
	M ₁	75.00	72.00	80.00	145.0	185.0	150.0	70.00	80.00	70.00
	M ₃	475.0	475.0	505.0	500.0	513.0	513.0	468.0	470.0	468.0
	\bar{U}	27.79	29.10	27.15	22.36	11.61	24.09	27.79	28.44	28.44
	A	.103	.097	.105	.215	.370	.210	.098	.110	.097
	I	86.00	86.00	85.50	83.75	81.75	83.75	85.75	86.75	86.50
	M ₁	85.00	65.00	62.00	98.00	145.0	105.0	70.0	65.00	62.00

Table 4. (Continued)

X (in)		Y (in)								
		-4	-3	-2	-1	0	1	2	3	4
11	M_3	410.0	410.0	408.0	420.0	428.0	425.0	450.0	415.0	408.0
	\bar{U}	26.52	26.52	25.90	21.26	17.16	21.26	25.9	28.44	27.79
	A	.106	.106	.103	.174	.288	.185	.105	.101	.099
16	I	87.00	86.50	85.50	83.50	83.25	84.25	84.50	86.75	86.75
	M_1	75.00	85.00	85.00	115.0	170.0	115.0	85.00	90.00	75.00
	M_3	465.0	465.0	465.0	485.0	490.0	485.0	470.0	472.0	465.0
	\bar{U}	29.10	27.99	25.29	20.71	20.18	22.36	22.93	28.44	28.44
	A	.103	.120	.122	.179	.266	.173	.129	.124	.111
21	I	86.00	86.50	85.50	84.00	83.50	84.25	85.50	85.25	86.75
	M_1	85.0	85.0	105.0	150.0	155.0	150.0	105.0	80.00	80.00
	M_3	465.0	485.0	485.0	480.0	480.0	480.0	485.0	470.0	472.0
	\bar{U}	26.52	27.79	25.29	21.80	20.71	22.36	25.29	24.68	28.44
	A	.122	.117	.143	.219	.254	.208	.151	.188	.110